

Poster Reprint

ASMS 2019
WP-444

Impact of Dwell Time and Ion Flux on Multiple Reaction Ion Monitoring (MRM) Measurement Precision

Behrooz Zekavat, Charles Nichols, Anabel Fandino

Agilent Technologies Inc., Santa Clara, CA

Introduction

Triple quadrupole mass spectrometers (TQ MSs) coupled to separation techniques are used for targeted quantitation of various analytes in different sample matrices with high specificity and sensitivity.

Due to the increased need for higher throughput and lab productivity as well as more demanding regulatory requirements, laboratories are monitoring an increased number of analytes using shorter chromatographic runs. As a result, more MRM transitions are monitored simultaneously per method at reducing dwell times. Therefore, it is important to understand the impact of dwell time and ion flux on the analytical assay precisions.

Here, the importance of MRM dwell time and ion flux on measurement precision and instrument detection limit is discussed and recommendation is provided for judicious selection of dwell times when developing LC-MS/MS assays.

Experimental

Direct Infusion MRM Data Acquisition and Analysis

A newly developed Agilent LC/TQ was used for the measurements reported in here. Agilent tune mix solution in direct infusion mode was used to characterize the impact of ion flux on measurement precision. Data at various ion flux were collected using either a standalone tool at 16-microsecond time resolution with no signal averaging and subjected to statistical data analysis for RSD calculation and pulse height distribution.



Figure 1. Agilent 6495C Triple Quadrupole Mass Spectrometer.

Experimental

LC-MS/MS Data Acquisition

LC-MS/MS data were collected using Agilent 1290 LC systems coupled to 6495C LC/TQ.

Peak Area Precision Measurements at Fixed Amount On-Column: Purpose of these measurements was to investigate the LC-MS/MS peak area precision as a function of dwell time. A total of ~190 MRM transitions from Agilent pesticide submixes 2, 4, and 7 were monitored at 20-pg on-column at each dwell time. LC-MS/MS data were collected using six different time segment methods at dwell times 0.5, 1.0, 3.0, 5.0, 10, or 15 ms. Cycle times were adjusted in the range of ~500 to 600 ms for each time segment and independent of dwell time. It was important to keep the cycle time independent of dwell times to eliminate the potential relative standard deviation (RSD) contribution from chromatographic peak integration which may arise from discrepancy of the number of data points across the LC peaks. RSD values were calculated from 10 replicate injections and no smoothing was applied to LC-MS/MS chromatograms. RSD values were calculated from 10 replicate injections.

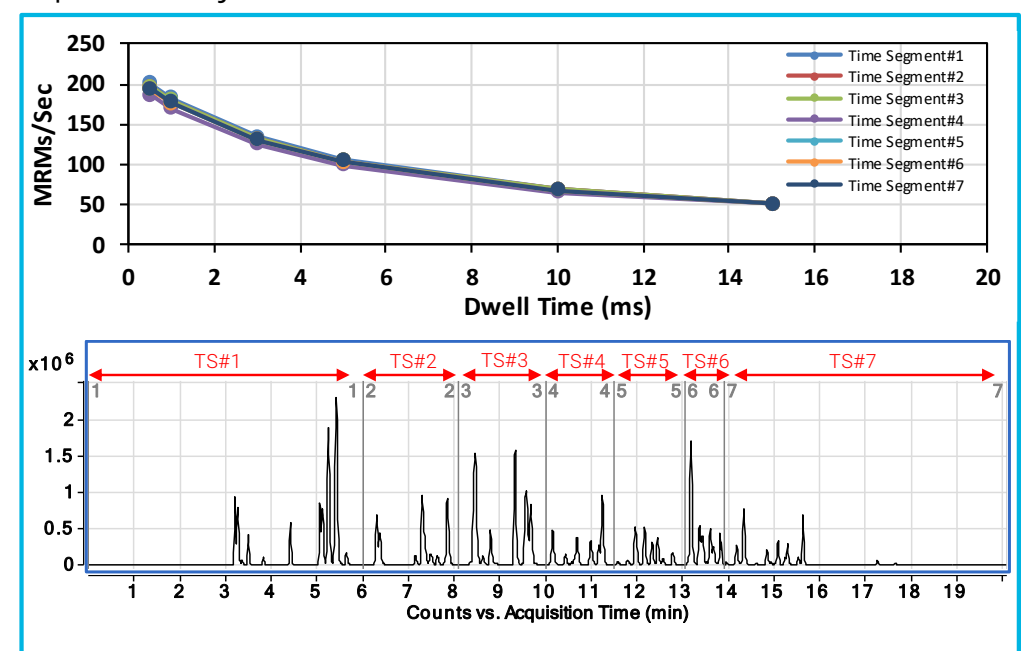


Figure 2. Top panel: MRM acquisition speed as a function of dwell time for the time segment (TS) method data collection. Bottom panel: Representative time segment TIC at dwell time 15 ms.

Peak Area Precision Measurements at Varied Amount On-Column: Purpose of these measurements was to estimate the impact of dwell time on instrument detection limit (IDL) at dwell times 0.5, 1.0, 3.0, 5.0, and 15 ms. A total of five analytes including acetaminophen, caffeine, sulfaguanadine, sulfadimethoxine, and Val-tyr-val were used at amounts on-column ranging from 10 fg to 10,000 fg. MRM method cycle time was adjusted at ~500 ms and independent of dwell time.

Theoretical Background

One of the well known random effects that influences mass spectrometers' analytical performance is non-systematic fluctuation of ion beam generated at the ion source. This random process is governed by a discrete probability distribution, known as Poisson distribution, for an analyte introduced into the mass spectrometer inlet at a constant rate (=number of ions introduced per time interval) [1]:

$$P(n) = v^n e^{-v} / n! \quad \text{Equation (1)}$$

"v" is the average number of ions per time interval and "P(n)" is the probability of obtaining "n" counts as the outcome of a particular measurement.

According to Equation 1, if one were to measure the average ion flux of an ion beam from an analyte into a mass spectrometer inlet, one would observe that each individual measurement randomly fluctuates about the mean. Statistically, this variation can be described as a Poisson process and minimum best RSD of any measurement made on the ion beam can be estimated using:

$$\text{RSD} = \text{Sqrt}(v) / v = 1/\text{Sqrt}(v) \quad \text{Equation (2)}$$

Assuming a fixed time interval, RSD[%] can be calculated according to:

$$\text{RSD} [\%] = 100 * [1/\text{Sqrt}(\text{Number of Ions})] \quad \text{Equation (3)}$$

Ions reaching to the detector generate output current that statistically fluctuate with Poisson distribution and RSD similar to Equation 3. Assuming that the two above-mentioned ion signal fluctuation are independent, the total best RSD can be estimated by error propagation:

$$\text{RSD} [\%] \approx 100 * [\text{Sqrt}(2/(\text{Number of Ions}))] \quad \text{Equation (4)}$$

More ions means reduced RSD or less noise and random fluctuation in the measurements. Note that this relationship assumes no change in event rate (or number of ions introduced per time interval) and is valid for low ion counts. The stochastic nature of measurements become less relevant at high ion counts.

Ion Signal RSD as a Function of Ion Flux

Figure 3, top panel shows typical random fluctuations at varied ion flux for m/z 118 recorded in MRM capture [2]. Examples of pulse height distributions are shown in middle panels. For comparison purpose, data in middle panels are normalized to the average counts for each data set. The resulting RSD values obtained from data in top panel are shown in bottom panel. Ion signal fluctuations in top panel represent the maximum signal RSD at the corresponding ion flux without any signal averaging. In a typical MRM data acquisition, ion signal is averaged over a period of "dwell" time.

As shown in Figure 3, the signal RSD increases as the ion flux decreases. This increase in signal RSD at low ion signal will have a direct impact on the observed peak area RSD in a typical MRM assay as it is discussed in the next sections.

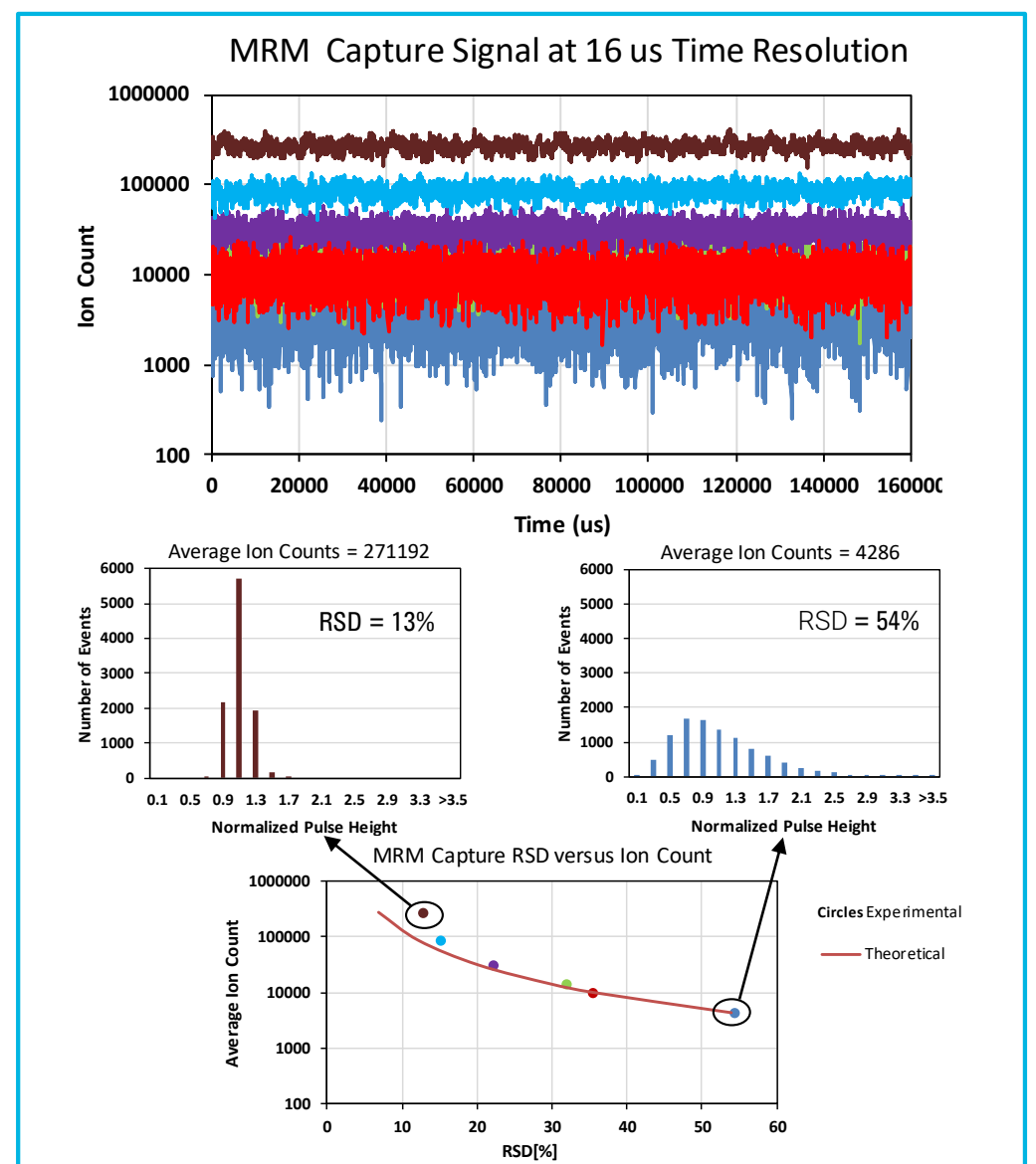


Figure 3. Top panel: Experimentally measured MRM capture signal at m/z 118 depicting random fluctuation of ion signal as a function of ion beam intensity. Middle panel: Pulse height distribution of two ion signal traces shown in top panel. X axes are the normalized data for each distribution. Bottom panel: Experimentally calculated RSD values for ion signal traces shown in top panel. Red solid lines in the bottom plots are the theoretical RSDs based on ion statistics.

LC-MS/MS Area RSD at Varied Dwell Time and Ion Flux

Figure 4 shows the distribution of peak area RSD[%] for a mixture of pesticides at different dwell times. Pesticides in this mixture cover a wide range of area responses corresponding to different number of ions reaching to detector. Plots of peak area versus RSD shows separate “trend line” for the data set at each dwell time. Further inspection of these plots reveals that: (i) peak area RSDs increase with decreasing area responses (or number of ions) and (ii) a larger RSD change per area response change for data sets at shorter dwell times as compared to longer dwell times.

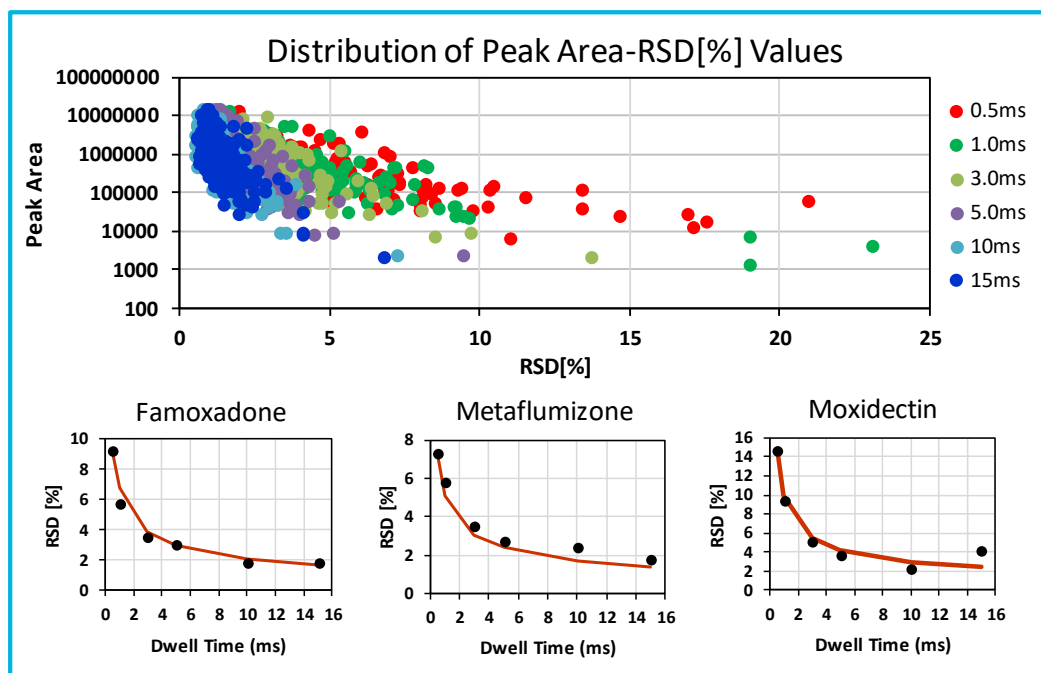


Figure 4. LC-MS/MS peak area vs. RSD at various dwell times for a mixture of pesticides. Red solid lines in the bottom plots are theoretical RSDs based on ion statistics.

Figure 5 shows representative MRM chromatographic peak shapes at dwell time = 0.5 and 15 ms. The two pesticides in Figure 5 have different area responses (at 20pg on-column) due to their ionization efficiency differences which results in lower ion flux for rimsulfuron as compared to tricyclazol. Impact of the ion flux on peak shape is more evident at dwell time = 0.5 ms for tricyclazole with lower peak area. Tricyclazole with higher area response shows indistinguishable peak shapes at dwell times = 0.5 and 15 ms.

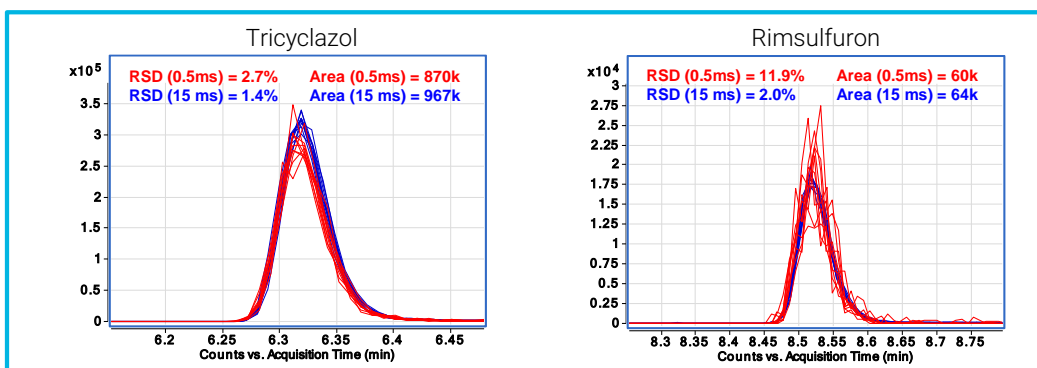


Figure 5. Overlaid MRM chromatograms (10 replicates) for two pesticides with ~10x difference in are response at short and long dwell times. No smoothing applied.

Instrument Detection Limit at Varied Dwell Time

Data in Figure 6 demonstrate how instrument detection limit is influenced by dwell time. To collect the data in Figure 6, various amount on-column for each analyte was injected and RSDs were calculated at each dwell time.

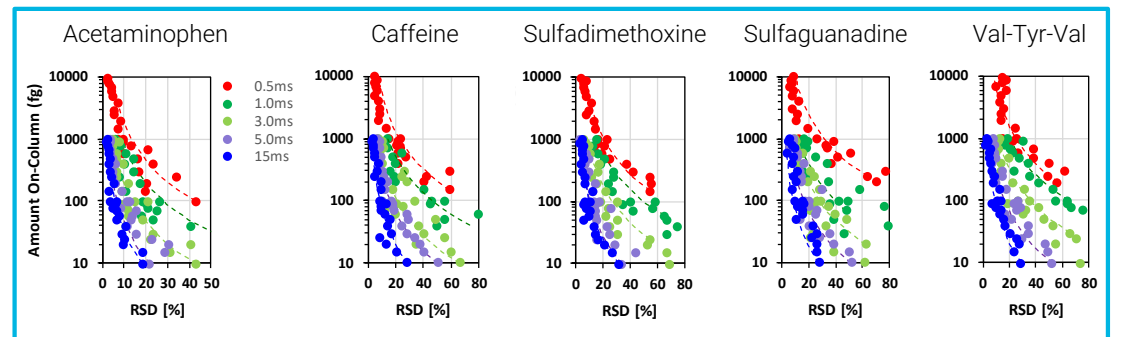


Figure 6. LC-MS/MS peak area RSD as varied amounts on-column and dwell times.

Summary of IDL values at various dwell times for the five tested analytes is shown in Table 1. IDL values were calculated at 98% confidence level and at the lowest amount on-column to reach a RSD[%] of ~15-20%. As shown in Table 1, achievable IDL for each analyte is a function of dwell time and becomes worse at shorter dwell times.

Table 1. Estimated IDL values at different dwell times*.

Analyte	0.5 ms		1.0 ms		3.0 ms		5.0 ms		15 ms	
	RSD [%]	IDL (fg)	RSD [%]	IDL (fg)	RSD [%]	IDL (fg)	RSD [%]	IDL (fg)	RSD [%]	IDL (fg)
Acetaminophen	13.2	297	18.3	51.6	18.3	25.9	15.3	13.0	18.2	105.1
Caffeine	14.5	423	19.7	111	20.8	52.9	16.6	46.8	15.6	22.0
Sulfadimethoxine	15.2	428	15.5	262	21.7	91.8	16.3	45.9	15.6	11.0
Sulfaguanadine	11.7	330	14.7	249	21.1	178.3	13.7	77.5	14.7	24.8
Val-Tyr-Val	13.5	762	18.8	531	23.0	129.8	11.3	32.0	16.3	18.4

* The reported values are only to show the impact of dwell time under identical LC gradient and MS parameters and not to be used as a reference.

Conclusions

- Both ion flux and dwell time impact the LC-MS/MS measurement precision.
- Similar ion flux results in lower assay precision at shorter dwell time.
- Fast MRM and dMRM acquisition rates utilizing short dwell times negatively impact the detection limit of LC-MS/MS assays.
- Plots of peak area-RSD[%] can be used to establish the target MRM dwell times based on the analyte response and desired area precision at the early stage of method development.

References

- 1H. N. Lee, A. G. Marshall, Anal. Chem. 2000, 72, 2256.
- 2B. Zekavat, L. L. Pollum, H. Wang, H. Nguyen, H. Bui, S. E. Tichy, ASMS 2018, San Diego, CA, MP-387.